



GravProcess: An easy-to-use MATLAB software to process campaign gravity data and evaluate the associated uncertainties



Rodolphe Cattin*, Stephane Mazzotti, Laura-May Baratin

Laboratoire Géosciences Montpellier, UMR 5243, Université Montpellier 2, Place E. Bataillon, 34095 Montpellier, France

ARTICLE INFO

Article history:

Received 17 September 2014

Received in revised form

10 April 2015

Accepted 11 April 2015

Available online 14 April 2015

Keywords:

Gravity data processing

Terrain correction

Tide correction

Gravity anomaly

ABSTRACT

We present GravProcess, a set of MATLAB routines to process gravity data from complex campaign surveys and calculate the associated gravity field. Data reduction, analysis, and representation are done using the MATLAB Graphical User Interface Tool, which can be installed on most systems and platforms. Data processing is divided into several steps: (1) Integration of gravity data, station location, and gravity line connection input files; (2) Gravity data reduction applying solid-Earth tide and instrumental drift corrections and, depending on the required processing level, air pressure and oceanic tidal corrections; (3) Automatic network adjustment and alignment to absolute base stations; (4) Free air and terrain corrections to calculate gravity values and anomalies, and to estimate the associated errors. The final step is dedicated to post-processing and includes graphical representations of data and an output text file, which can be used by Geographic Information System software. An example of this processing chain applied to a recent survey in northern Morocco is given and compared with previous available results.

© 2015 Elsevier Ltd. All rights reserved.

1. Introduction

Relative gravimeters are extensively used in numerous geoscience applications, including oil and mineral explorations (Aghajani et al., 2011), water storage (Deville et al., 2013), volcanology (Jousset et al., 2003), geothermal monitoring (Hunt and Kissling, 1994) or geodynamical studies (Berthet et al., 2013), thanks to their convenient field design and high precision. For instance, the “Scintrex Autograv CG-5” gravimeter can measure relative gravity variations with a standard deviation as low as 5 µGal (i.e. 50 nm s⁻²) in a quiet environment. In order to reach such a high-resolution, a mean gravity value and its standard deviation are computed from measurements at 1–10 Hz sampling rate and can be corrected in real-time for tilt, temperature, Earth tide, seismic noise, and instrument drift (Scintrex Operation Manual, 2014).

These real-time corrections are useful to provide first-order results in the field but cannot be used for high accuracy or multi-gravimeter projects (Gabaldá et al., 2003). The first-order models used for instrument drift and solid-Earth tide corrections, as well as the lack of correction for ocean tide and barometric pressure, limit the real-time measurement precision to 10–20 µGal (Longman, 1959; Merriam, 1992). Thus, post-processing and more complete data corrections are required for high accuracy results. In

addition to data correction, network adjustments and ties to an absolute gravity reference system are required to combine multiple acquisitions and compute gravity anomalies. These data reduction procedures also require post-processing and need to be carefully evaluated to estimate the associated uncertainties that propagate into the final data.

In this study, we present the GravProcess software, which is dedicated to computing high-resolution data associated with complex gravity surveys, following previous efforts to develop similar processing software (e.g., CG3TOOL; Gabaldá et al., 2003). This code is developed solely using the MATLAB language. This allows the user to perform all processing steps without the need for external software. Taking advantage of the MATLAB graphics toolbox, GravProcess can be installed on most systems and platforms. After presenting the general features of the program, we describe the corrections and adjustments applied to obtain a final gravitational field. We discuss the calculation of free air and Bouguer anomalies with a special emphasis on terrain correction. We next describe and discuss the calculation of the uncertainties associated with corrections and adjustments of gravity data. Finally, the processing of a recent survey in Morocco is shown for illustration.

2. Gravity field and gravity anomalies

The processing tasks are carried out through an easy-to-use and flexible graphical interface (Fig. 1). It allows the user to

* Corresponding author. Fax: +33 4 67 14 49 51.

E-mail address: cattin@gm.univ-montp2.fr (R. Cattin).

STEP 1 – INPUT FILES

Lines and calibration coefficient file ? (NoLINE COEFFICIENT)	<input type="text" value="lines.txt"/>				
Gravity data file (name after line number) ? (LINE STATION ALT GRAV GRAV_STD TILTX TILTY TEMPE TIDE DURATION REJECTED TIME DECIMAL_TIME TER DATE)	<input type="text" value="datagravi.txt"/>				
GPS location file ? (LON LAT ALT ALTITUDE_STD STATION)	<input type="text" value="GPSlocation.txt"/>				
Relative network adjustment file ? (LINE1 LINE2 LINE_attached(with respect to LINE2))	<input type="text" value="attachlist.txt"/>				
Absolute network adjustment file ? (LON_BASE LAT_BASE GRAVITY_BASE)	<input type="text" value="gravbase.txt"/>				
Complete Bouguer anomaly ?	<input checked="" type="checkbox"/> Yes	DEM file ? (LON LAT ALTITUDE)	<input type="text" value="DEM.xyz"/>	Mesh : Smin(km) dmax(km) alpha	<input type="text" value="0.1 200 0.2"/>
Ocean tide correction ?	<input checked="" type="checkbox"/> Yes	Ocean loading file ? (from H.-G. Scherneck)	<input type="text" value="oceantidal.txt"/>		
Pressure correction ?	<input checked="" type="checkbox"/> Yes	Pressure file ? (STATION PRESSURE TIME DATE)	<input type="text" value="pressure.txt"/>		
Parallel computing ?	<input checked="" type="checkbox"/> Yes	Drift: Degree of the polynomial function ?	<input type="text" value="1"/>	Uncertainty in the DEM (m) ?	<input type="text" value="0.5"/>

STEP 2 – RUN GRAVITY DATA PROCESSING

done

STEP 3 – OUTPUT

<input type="button" value="Plot results"/>	Output gravity data processing file ? (STATION LON LAT ALT GRAV GRAV_STD FREE-AIR FREE-AIR_STD BOUGUER BOUGUER_STD DATA_STD DRIFT_STD NETWORK_ADJUST_STD ABS_STD ALT_STA_STD DEM_STD)
<input type="button" value="Instrumental drift"/>	<input type="text" value="gravprocess.out"/>

Fig. 1. GravProcess main interface. Step 1 is dedicated to inputs and data files. In Step 2 gravity measurements are corrected and adjusted, and both free air and Bouguer anomalies are calculated. Step 3 corresponds to post-processing (graphical display and outputs).

(1) import various data files, (2) compute accurate and adjusted gravity station values and (3) plot corrected data and export results into a text file. The various processing tasks are shown in Fig. 2 and described below. They are performed by individual subroutines called independently from the graphical interface.

2.1. Importing data into GravProcess

Because this software is dedicated to processing data from complex surveys, we favor the use of input files rather than window-based data editing. Gravity data are organized by “lines”, which comprise measurements at stations associated with a unique gravimeter and drift estimate, i.e., typically acquired over one of two days (Fig. 3).

GravProcess requires at least five input files:

- a calibration file, with the gravimeter calibration factor for each line.
- raw gravity data files (one per line) in the Scintrex CG5 format.

- a stations location file providing longitude, latitude, elevation and elevation uncertainty for each gravity station.
- a network file that defines the sequence and steps of line combinations into an adjusted network.
- an absolute base station file with locations and values of absolute gravity measurements for reference points.

Depending of the required accuracy, three additional files can be imported:

- a digital elevation model (DEM) to calculate terrain correction. This DEM must be referenced to the same ellipsoid as the station locations. Commonly, GPS locations are referenced to the WGS84 ellipsoid.
- an ocean tide correction file, with ocean-loading coefficients at chosen locations. This file can be obtained from the website <http://holt.oso.chalmers.se/loading/> developed by Bos and Scherneck,
- a barometric measurement file that contains the location, date

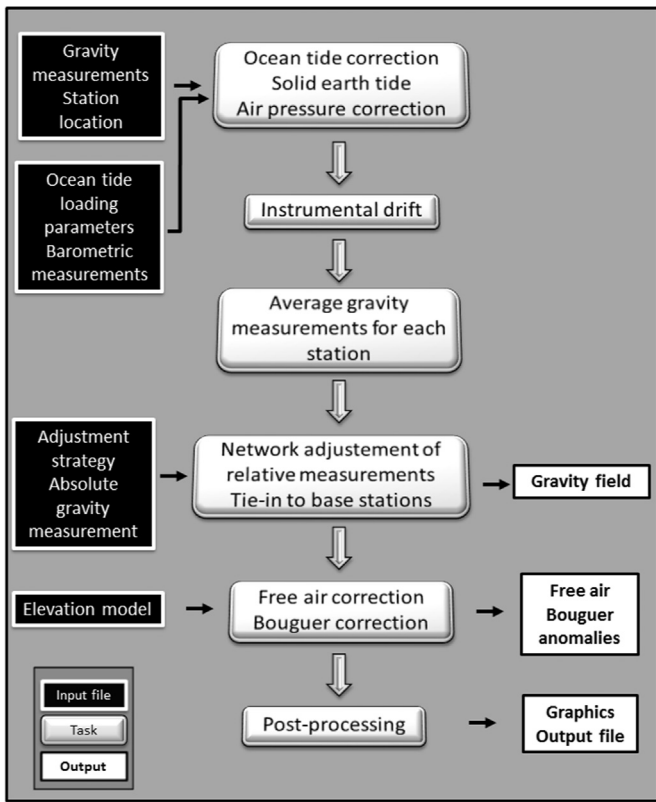


Fig. 2. Flow chart for gravity data processing. Black, gray and white boxes are associated with input file, data processing, and output, respectively.

and time of pressure measurements.

A detailed description of input file formats is provided in the user manual included in the GravProcess software package.

2.2. Reduction of raw data

Field data reduction (Earth and ocean tides, pressure and instrument correction) and network adjustment are applied to each line using the following procedure. As a first step, raw measurements with a standard deviation greater than 0.2 mGal are discarded (cf. user manual to modify this threshold value).

2.2.1. Earth and ocean tide corrections

The first temporal effect to be corrected is tidal deformation of both solid-Earth and ocean-loading. These corrections are carried out for each measurement using their specific time information. For both corrections, GravProcess routines are based on Fortran codes developed by Agnew (2007, 2012), which we translated into MATLAB. The solid-Earth tide correction is a direct computation of the tidal potential following the development proposed by Munk and Cartwright (1966). It is based on internal tidal parameter sets, especially an ephemeris, i.e. a description of the location of both the Moon and Sun in celestial coordinates. With a maximal error of 0.5 µGal, this non-harmonic method is very convenient to remove solid-Earth tide from gravity measurements (Van Camp, 2003).

Ocean tide correction is computed from loading parameters for the semidiurnal (M2, S2, N2, K2), diurnal (O1, P1, Q1, K1) and long-period (MF, Mm, Ssa) tidal harmonics (Agnew, 2012). The ocean-loading coefficients are not calculated with GravProcess but must be provided from an external source (Fig. 2), e.g. Scherneck's free ocean provider (<http://holt.oso.chalmers.se/loading/>). For each gravity measurement station, GravProcess uses the ocean-loading

coefficients from the nearest location in the input file (Fig. 2).

2.2.2. Pressure correction

The second temporal effect is associated with atmospheric pressure. Changes in atmospheric pressure imply changes in the mass of the air column above the gravity point of measurement. Thus, an increase (decrease) in atmospheric pressure will cause a decrease (increase) in observed gravity. These changes are significant for microgravity surveys. Following the approach proposed by Gabalda et al. (2003), pressure correction is applied using the analytical formulation of Torge (1989):

$$\text{pressure correction} = C_p \times (P_z - P_0), \quad (1)$$

where $C_p = 0.3 \mu\text{Gal hPa}^{-1}$ is a linear coefficient for pressure correction, and P_z and P_0 are the atmospheric pressure at station elevation z during gravity measurements and reduced to sea level, respectively. For elevation expressed in meters and pressure in hPa, the pressure reduced to sea level is (Torge, 1989):

$$P_0 = 1013.25 \times \left(1 - \frac{0.0065 \times z}{288.15}\right)^{5.2559}. \quad (2)$$

2.2.3. Instrumental drift correction

Correction of gravimeter drift plays a significant part in the accuracy of all gravity surveys because it can reach up to 1 mGal/day. In GravProcess, drift is sampled at base stations with repeated measurements. The main advantage is that loops are not required, i.e., the base stations need not be the start or end points of lines. For each line, this base station is defined as the station with the longest time interval between repeated measurements (Fig. 3a). Drift is estimated by a least-square fit of the weighted time series at this station with an n th order polynomial function. The weighting factor used is the inverse of the standard deviation associated with each measurement. In many cases, a first-order polynomial function is enough to remove short-term instrumental drift for lines with duration between hours and a couple of days (Fig. 4). For longer duration, a polynomial function of higher order can also be applied to remove non-linear instrumental drift.

2.2.4. Mean gravity measurement

Typically, reduction of noise caused by human activity, wind or ocean waves is obtained by averaging gravity values recorded at 1–10 Hz sampling frequency over 1–2 min, yielding a gravity value g with its standard deviation σ_g for the station. These measurement sets are commonly repeated several times at the same location. Thus, the assessment of the gravity field at each station requires estimating the combined mean of N set values (themselves means of high-frequency measurement). Here, the final gravity value at a station g_{obs} is defined as the average of g :

$$g_{obs}(\text{station}) = \frac{1}{N} \sum_{i=1}^N g_i(\text{station}). \quad (3)$$

2.3. Network adjustment

A typical gravity survey network is a set of interconnected lines and reference stations. After tide, pressure, and instrumental drift corrections have been applied to the raw gravity data, the corrected values correspond to series of relative gravity values, which need to be adjusted to a common reference given by absolute reference points.

Here, these network adjustments are done in two steps. The first one consists in successive adjustments of pairs of gravity lines defined by the user in the network adjustment file (Fig. 3b). This simple approach is efficient for complex surveys, especially in case

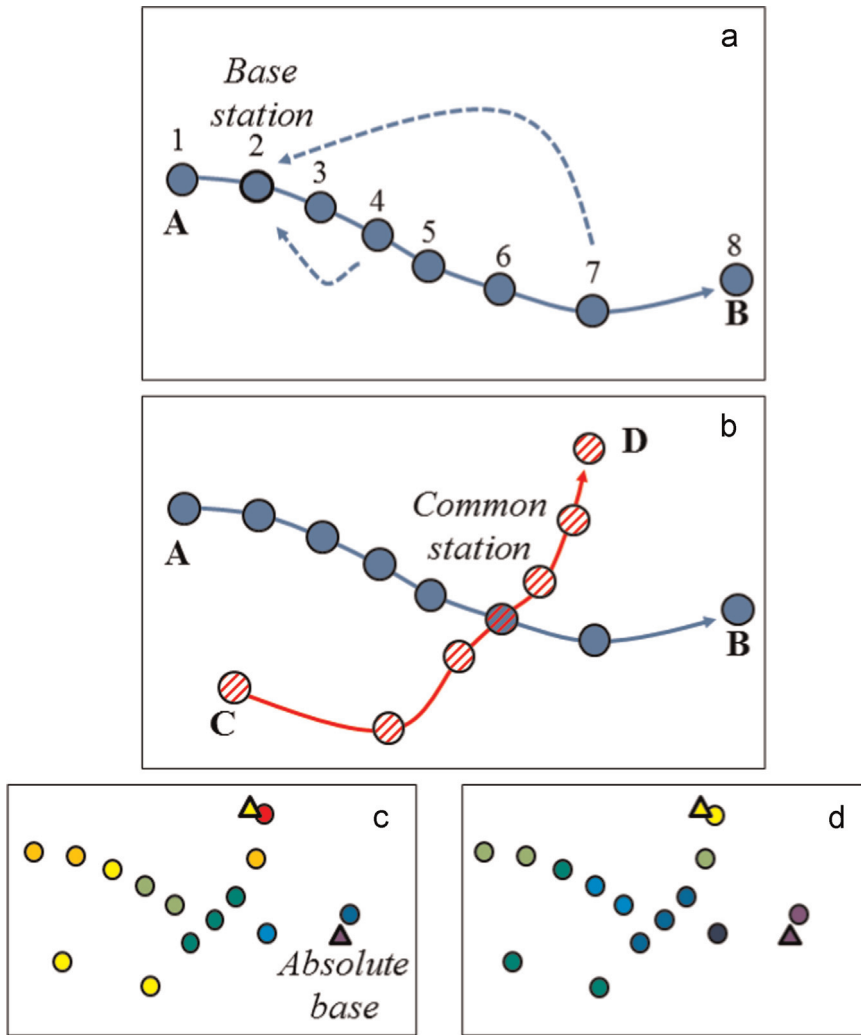


Fig. 3. Gravity measurements and network adjustment. Circles and triangles correspond to relative and absolute gravity measurements, respectively. (a) A line consists in gravity measurements over one or two days at stations associated with a unique gravimeter and drift estimate. Here we consider the line "AB", which consists in 10 gravity measurements at 8 stations. Instrumental drift is estimated from repeated measurements at the base station 2. (b) Adjustment of pairs of gravity lines ("AB" and "CD") is obtained by averaging the differences of gravity values at stations common to both lines. (c) Adjusted gravity network, for which all gravity measurements are relative to a same reference. (d) Adjusted and shifted gravity network, for which all gravity measurements are tied to one or more absolute base stations.

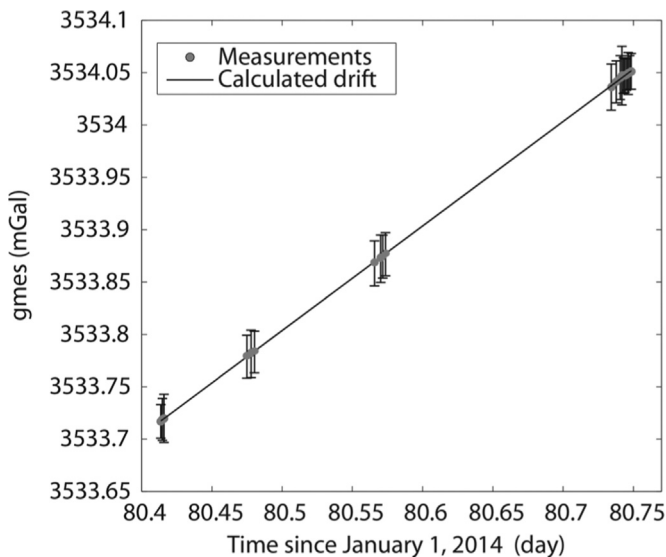


Fig. 4. Example of instrumental drift calculation. Gray circles with error bar show individual gravity measurements. Black line is the estimated drift.

of lines that interconnect with each other via different paths. For each line pair, the adjustment is obtained by averaging the differences of gravity values at stations common to both lines. The adjusted set is then recorded in a temporary line that can be used for further adjustment. An example, of network adjustment is given in Table 1: lines "AB" and "CD" are adjusted together in a new line "ABCD" (Fig. 3b and c), lines "EF" and "GH" in new line "EFGH", lines "ABCD" and "EFGH" in new line "0". Line 0 corresponds to the final one, for which all gravity measurements are relative to a same reference.

This relative network is shifted in a second step, which is dedicated to the tie of the relative measurements to one or more

Table 1

Example of network adjustment file (see Fig. 3). The first two columns give the name of the two lines that are adjusted together. The third column gives the name of the resulting adjusted line.

Input line 1	Input line 2	Output line
AB	CD	ABCD
EF	GH	EFGH
ABCD	EFGH	0

absolute base stations (Fig. 3c and d). In many cases, absolute base stations and relative measurements are not at the exact same location. Thus, the shift is defined as the mean of the differences in gravity values between each absolute base station and the closest campaign station.

2.4. Free air and Bouguer anomaly

The free air FA and Bouguer BA anomalies are calculated from the following equations:

$$\begin{cases} FA = g_{obs} - (g_{th} - \text{correction}_{\text{free air}}) \\ BA = g_{obs} - (g_{th} - \text{correction}_{\text{free air}} + \text{correction}_{\text{Bouguer}}) \end{cases} \quad (4)$$

where g_{obs} are the corrected and adjusted gravity measurements and g_{th} the theoretical gravity field on the reference ellipsoid. The free air correction expressed in mGal is:

$$\text{correction}_{\text{free air}} = 0.3086 \times h \quad (5)$$

with h the elevation in meter above the ellipsoid.

Depending on the required accuracy the user can choose between a simple or complete Bouguer reduction. The simple one is calculated from the plateau formulation:

$$\text{correction}_{\text{Bouguer}} = 2 \times \pi \times \rho \times G \times h \quad (6)$$

where ρ is the density (2670 kg m^{-3} by default, cf. user manual for modification) and $G=6.67 \times 10^{-11} \text{ N m}^2 \text{ kg}^{-2}$ is the gravitational constant.

A complete Bouguer correction is also proposed to account for local irregularities in topography around gravity stations. GravProcess use a DEM combined with the station location file, which provides the elevation at the gravity station with a better accuracy. The terrain correction can integrate land, marine, airborne, and satellite data that need not be on a regular grid. It is computed from the MATLAB routines developed by Singh and Guptasarma (2001), which gives the gravity field due to a solid body bounded by plane surfaces and having uniform density. Here, to account for the mixed topography and bathymetry DEM, we assume two solid bodies with densities of 2670 kg m^{-3} and 1000 kg m^{-3} , respectively.

For topography, the body surface is defined using the following approach:

1. The elevation of points below sea level is fixed to 0 m.
2. The resulting DEM is then meshed into triangles with higher density near the stations. This local grid refinement is performed using the MATLAB mesh2D tool developed by Engwirda. In addition to this automatic setting, the user can specify the mesh resolution at the station s_{min} , the radius of the used area d_{max} and the coefficient α that controls the relaxation of the mesh size s with the distance d from the station according to:

$$s = s_{min} + \alpha \times d_{|d < d_{max}} \quad (7)$$

3. These triangles are then used to define the upper body surface.
4. The bottom surface is defined by the same triangles with an elevation 0 m.
5. Four vertical faces are used to close the body surface.

For seawater, a similar approach is used except that bathymetry data define the bottom surface. Top surface then corresponds to sea level.

3. Evaluating error associated with data and processing

In order to estimate the standard errors on the final gravity field and anomaly values, the uncertainties associated with all processing levels are estimated and propagated at each step by adding the variances. Thus, each processing step takes into account the cumulated uncertainties up to that level. First-order solid-Earth, oceanic and atmospheric pressure corrections applied in GravProcess are associated with very low uncertainties (few to few tens of μGal ; e.g., Merriam, 1992; Baker and Bos, 2003) and are neglected in our error analysis. Other steps are described below.

3.1. Drift correction

The polynomial function $\sum_{i=0}^n a_i t^i$ used to estimate instrumental drift with time t is associated to a covariance matrix $\text{cov}(a_i, a_j)$ for the drift coefficients a_i , which can be used to assess the uncertainty $\sigma_{\text{drift correction}}$ due to this correction:

$$\sigma_{\text{drift correction}}^2 = \sum_{i=0}^n \Delta t^{2i} \text{cov}(a_i, a_i) + 2 \sum_{i,j:i < j} \Delta t^i \Delta t^j \text{cov}(a_i, a_j), \quad (8)$$

with Δt the longest time interval between repeated measurements at a base station. For instance, with a linear drift given by $a_1 \times t + a_0$, the standard deviation can be written as:

$$\sigma_{\text{drift correction}} = \sqrt{\Delta t^2 \text{cov}(a_1, a_1) + 2\Delta t \text{cov}(a_1, a_0) + \text{cov}(a_0, a_0)}, \quad (9)$$

3.2. Gravity measurements

The gravity field at each station results from the combination of N measurements g with their own standard deviation σ . We use the following formulation for the combined uncertainty (Jousset et al., 1995):

$$\sigma_{\text{obs}} = \sqrt{\left[\frac{1}{N} \sum_{i=1}^N (g_i^2 + \sigma_i^2) \right] - g_{\text{obs}}^2}, \quad (10)$$

where g_{obs} is the final gravity value at a station (Eq. (3)).

3.3. Network adjustment

The network adjustment is based on the differences between sets of gravity data. The resulting uncertainty is calculated by taking the geometric average of the standard deviations of stations common to both sets. One can note that changing the order of these adjustments does not change the result. Thus, rather than propagating the error from one line to the next into the network, we assume a uniform uncertainty $\sigma_{\text{relative adjustment}}$, which corresponds to the average standard deviation obtained for all line pairs.

The error $\sigma_{\text{absolute adjustment}}$ associated with the tie to one or more absolute base stations can be estimated as the standard deviation of differences between the measurements at the base stations and the referenced measurements at the closest relative stations. The resulting standard deviation associated with the total network adjustment is:

$$\sigma_{\text{network adjustment}} = \sqrt{\sigma_{\text{relative adjustment}}^2 + \sigma_{\text{absolute adjustment}}^2}. \quad (11)$$

3.4. Free air and Bouguer corrections

The uncertainty in mGal associated with the free air correction is simply:

$$\sigma_{\text{free air}} = 0.3086 \times \sigma_t, \quad (12)$$

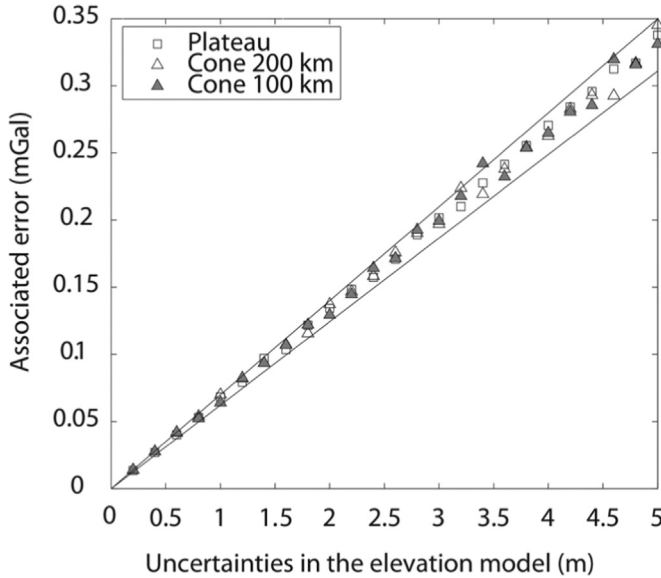


Fig. 5. Estimated terrain correction error associated with uncertainties in the Digital Elevation Model (DEM). Squares and triangles give the result for a plateau and a cone-shape elevation model, respectively. White (gray) triangles are related to a conic base of 200 km (100 km). Correlation coefficients of 0.06–0.07 between DEM uncertainties and the resulting terrain correction error are shown with the two solid lines.

with σ_h the station elevation uncertainty expressed in meters.

The Bouguer correction can generate two types of uncertainties. First, uncertainties in the elevation model σ_{DEM} can lead to error in the terrain corrections $\alpha_{terrain-DEM}$. Second, the parameters s_{min} , d_{max} and α used in the grid definition can modify the effect of irregularities in topography around gravity stations. To study these effects we use two simple elevation models, which consist in a 1 km high plateau and a cone with a maximum elevation of 1 km and a base diameter w_{cone} .

$\alpha_{terrain-DEM}$ is calculated at the top of a plateau and two cone models ($w_{cone} = 200$ and 100 km) to which a random perturbation is added. This perturbation is generated from a normal distribution with a standard deviation σ_{DEM} ranging from 0.2 to 5 m. Our results suggest a linear relationship for all tested models (Fig. 5):

$$\alpha_{terrain-DEM} = \beta \times \sigma_{DEM}, \quad (13)$$

with $\beta = 0.06\text{--}0.07$ for $\alpha_{terrain-DEM}$ and σ_{DEM} expressed in mGal and m, respectively.

In the previous tests we have assumed $s_{min} = 0.1$ km, $d_{max} = 200$ km and $\alpha = 0.2$. To assess the error $\alpha_{terrain-mesh}$ due to variations in these parameters we consider two elevation models (a plateau and a cone with $w_{cone} = 200$ km) for which $\sigma_{DEM} = 0$ m. These two models are meshed with s_{min} ranging from 0.05 to 5 m, d_{max} from 50 to 500 km and α from 0.1 to 1 (Fig. 6). As expected for a plateau flat topography, $\alpha_{terrain-mesh}$ is only controlled by d_{max} (Fig. 7a). More interestingly, for a conic topography our results reveal a more complex distribution for $\alpha_{terrain-mesh}$ (Fig. 7b). First,

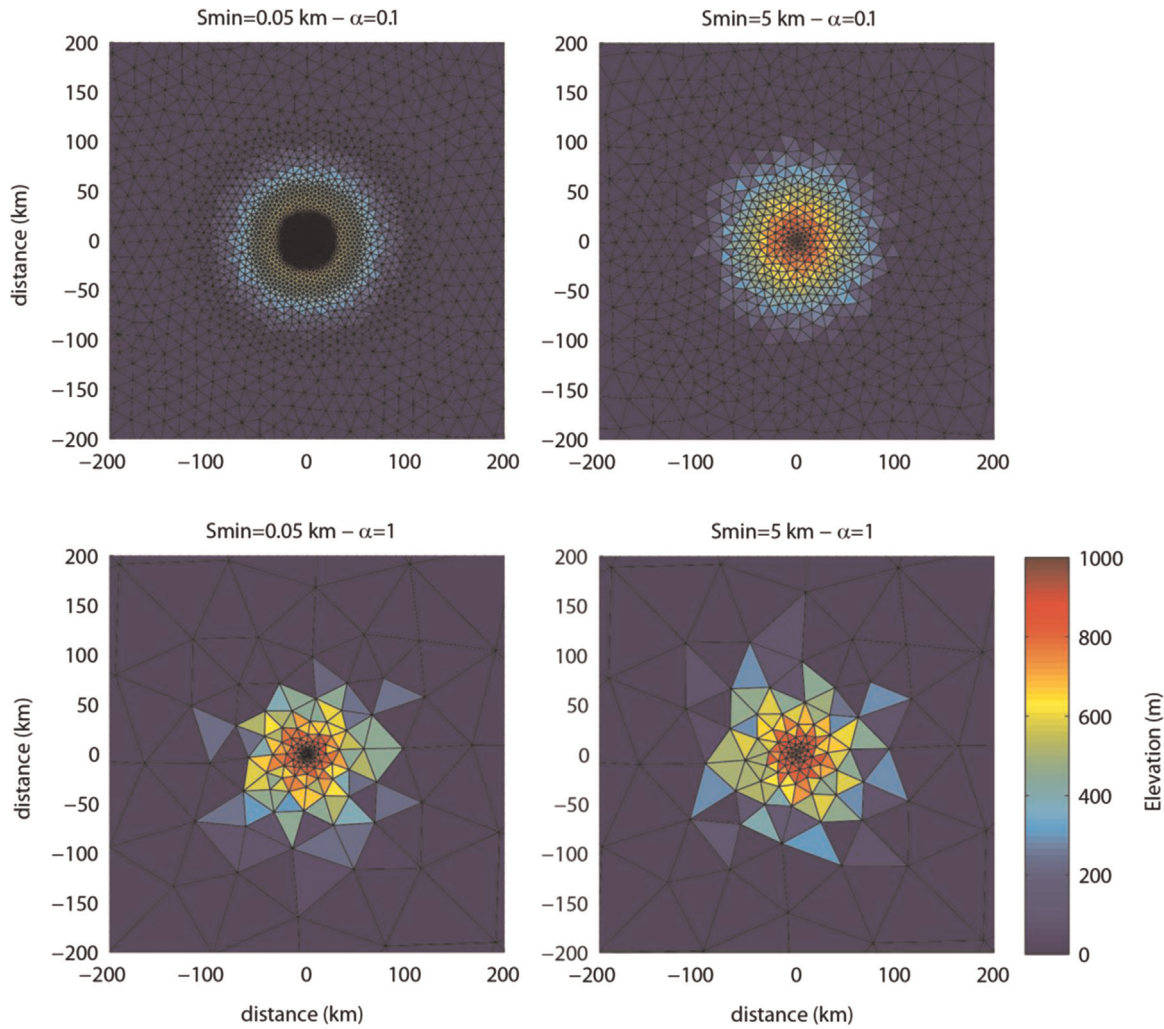


Fig. 6. Conic shape elevation model meshed with a resolution s_{min} of 0.05 and 5 km (left and right) and a coefficient α of 0.1 and 1 (top and bottom).

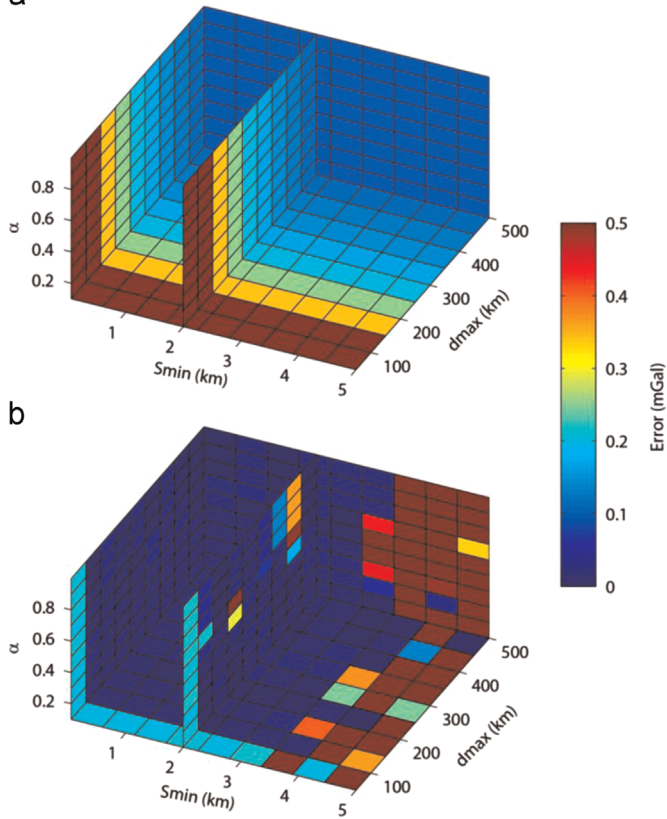
a

Fig. 7. Terrain correction uncertainties due to grid refinement associated with (a) a 1 km high plateau and (b) a 1 km high and 200 km diameter cone.

d_{\max} must be greater than 100 km, which corresponds to the radius of the conic base. Second, the resolution s_{\min} is a key threshold parameter, which must be lower than 2.5 km in these tests. Finally, compared to other parameters, α seems to play a minor role in the $\sigma_{\text{terrain-mesh}}$ distribution.

More complex elevation models must be tested to confirm these preliminary results. However this requires a systematic study of various wavelengths and surface roughness, which is out of the scope of the present paper. Based on our results, to limit the effect of mesh refinement and ensure that $\sigma_{\text{terrain-mesh}} < 0.1$ mGal, we favor the use of d_{\max} greater than the wavelength of the major topographic structures, s_{\min} equal to the best available DEM resolution and $\alpha = 0.2$.

4. Application to a test survey

GravProcess is illustrated using a relative gravity survey carried out in northern Morocco in the region between the Rif and Middle Atlas Mountains (Fig. 8) in March 2014. This campaign, dedicated to filling a hole in data available at the BGI (Bureau Gravimétrique International), was carried out by two teams using two Scintrex CG-5 gravimeters and dual-frequency GPS for elevation measurements. Each team measured gravity on daily closed lines with a minimum of one common point between the team lines and between consecutive days, for a total of 86 stations. Station data consisted in 8–10 sets of 90-s measurements at 6 Hz frequency. In order to provide absolute calibration, a subset of 3 stations was measured at points close to (< 0.2 km) previous surveys and available in the BGI database. This campaign dataset provides a useful test due to the strong variations in topography and relief (from 0 to 1600 m elevation), the large lateral gradient in gravity (Bouguer anomaly between 0 and -150 mGal), and the relatively

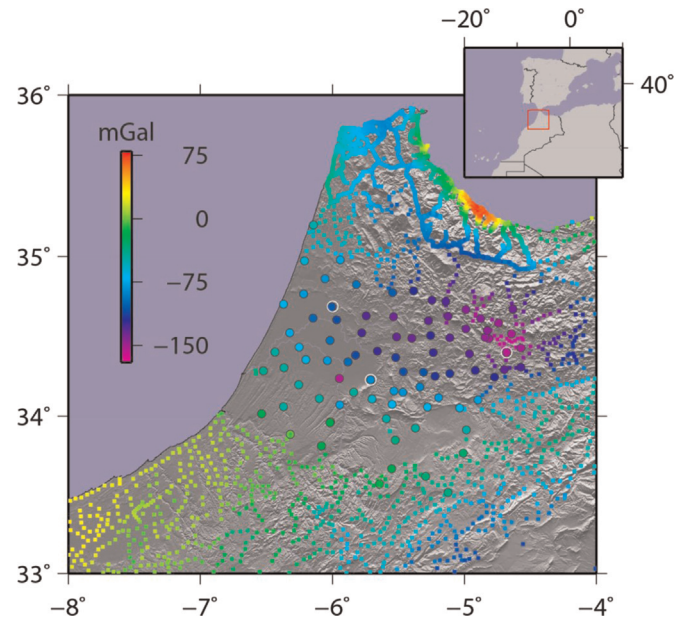


Fig. 8. Topographic map showing Bouguer anomalies in northern Morocco calculated with GravProcess (circles) and available from the BGI (squares). White circles indicate the location of base stations used in this study.

large distances between stations (10–20 km).

For this survey, uncertainties associated with instrument drift are small; $\sigma_{\text{drift correction}}$ is commonly equal to several μ Gal and can reach up to 0.045 mGal. Measurements with a standard deviation greater than 0.2 mGal are excluded from the data set, resulting in station uncertainties, $\sigma_{\text{measurement}}$, typically less than this value. The measurement uncertainty reaches 2.6 mGal for a couple of stations due to strong variations in their 8–10 measurement set. Assuming 0.3 m accuracy in the GPS vertical location leads to free air correction uncertainty $\sigma_{\text{free air}} = 0.09$ mGal. We use a DEM combining STRM on land and ETOPO2 offshore to calculate terrain correction. Assuming $\sigma_{\text{DEM}} = 5$ m leads to $\sigma_{\text{terrain-DEM}} = 0.3 – 0.35$ mGal. Using $d_{\max} = 200$ km, $s_{\min} = 0.11$ km and $\alpha = 0.2$, one can consider that $\sigma_{\text{terrain-mesh}} < 0.1$ mGal. Together, excepted for the two stations mentioned previously, these uncertainties lead to a low error (< 1 mGal) in the calculated Bouguer anomalies. The most significant source of error is due to the relative network adjustment to the three absolute gravity base stations. Due to the lack of actual absolute gravity data, we use absolute values estimated at previous campaigns from the BGI archive, which leads to a network adjustment with $\sigma_{\text{network adjustment}} = 2.5$ mGal. Overall, the combined uncertainty in Bouguer anomalies is estimated to ~ 2.8 mGal and reaches 5.1 mGal for the two anomalous points.

Processed data from the Morocco survey are in good agreement with those available from the BGI. Comparison of Bouguer anomalies over the region show that the new data integrate well within the pattern of very low values located between the Rif and Middle Atlas Mountains, with a regular increase from -150 to 0 mGal within ~ 100 km distance (Fig. 8). A subset of 4 data points near 34.2°N , -5.9°E show anomalous values that differ by 10 s of mGal compared to the neighboring stations. These points belong to the same line and are associated with uncertainties of ~ 2.6 mGal, similar to other lines and primarily due to network adjustment error, which points to acquisition problems for this specific line. A direct comparison of Bouguer anomalies from the new survey with those at BGI station within less than 5 km shows a good agreement (Fig. 9), with a mean (root-mean-square scatter) dispersion of 2.6 mGal. This level of difference, similar to the estimated uncertainties on the new data, is expected from the

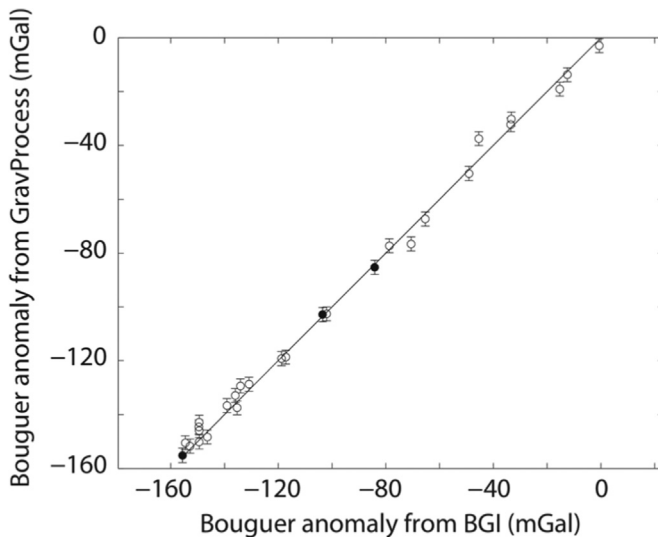


Fig. 9. Comparison between Bouguer anomalies calculated with the GravProcess program and those available from the BGI archive. The maximum distance between new and BGI points is 5 km. Black circles correspond to the three reference stations used in this study.

difference in processing and topography correction between the new data and the BGI data that were acquired and processed mainly in the 1960s.

5. Conclusion

GravProcess is a graphical interactive software to process campaign gravity data. It is especially dedicated to processing high-resolution data associated with complex gravity surveys that include large datasets, few loosely distributed absolute gravity measurements, or that involve multiple gravimeters and operators over many years. The code has been developed to easily perform data reduction (solid-Earth and ocean tide, instrument drift) and network adjustment, as well as calculate gravity anomalies and their uncertainties. The code is developed solely using the MATLAB language, which allows the user to perform all processing steps without the need for external programs.

Acknowledgements

Helpful reviews are provided by G. Hetényi and P. Jousset. We are grateful to N. Le Moigne for technical information concerning Scintrex CG-5 gravimeters, to D. Agnew for providing his tidal correction source codes, and to J. Chéry and A. Tahayt for their

participation in the Morocco gravity survey. This work was supported by grants from ANR (ANR-12-CHEX-0004-01), INSU-ALEAS and CNES-TOSCA.

Appendix A. Supplementary information

Supplementary data associated with this article can be found in the online version at <http://dx.doi.org/10.1016/j.cageo.2015.04.005>.

References

- Aghajani, H., Moradzadeh, A., Zeng, H., 2011. Detection of high-potential oil and gas fields using normalized full gradient of gravity anomalies: a case study in the Tabas Basin, Eastern Iran. *Pure Appl. Geophys.* 168 (10), 1851–1863.
- Agnew, D.C., 2007. Earth tides in treatise on geophysics In: Herring, T. (Ed.), *Geodesy*, vol. 3. Elsevier, Boston, pp. 163–195.
- Agnew, D.C., 2012. SPOTL: Some Programs for Ocean-Tide Loading Scripps Institution of Oceanography. SIO Technical Report. http://dx.doi.org/http://escholarship.org/uc/sio_techreport
- Baker, T.F., Bos, M.S., 2003. Validating earth and ocean tide models using tidal gravity measurements. *Geophys. J. Int.* 152, 468–485. <http://dx.doi.org/10.1046/j.1365-246X.2003.01863.x>
- Berthet, T., Hetényi, G., Cattin, R., Sapkota, S.N., Champollion, C., Kandel, T., Doerflinger, E., Drukpa, D., 2013. Lateral uniformity of India Plate strength over central and eastern Nepal. *Geophys. J. Int.* 195 (3), 1481–1493, first published online September 27. <http://dx.doi.org/10.1093/gji/ggt357>.
- Deville, S., Jacob, T., Chéry, J., Champollion, C., 2013. On the impact of topography and building mask on time varying gravity due to local hydrology. *Geophys. J. Int.* 192 (1), 82–93. <http://dx.doi.org/10.1093/gji/ggs007>.
- Gabalda, G., Bonvalot, S., Hipkins, R., 2003. CG3TOOL: an interactive computer program to process Scientex CG-3/3 M gravity data for high-resolution applications. *Comput. Geosci.*, 29; , pp. 155–171.
- Hunt, T.M., Kissling, W.M., 1994. Determination of reservoir properties at Wairakei geothermal field using gravity change measurements. *J. Volcanol. Geotherm. Res.* 63, 129–143.
- Jousset, P., Van Ruymbeke, M., Bonvalot, S., Diamant, M., 1995. Performance of two Scintrex CG3M instruments at the fourth International Comparison of Absolute Gravimeters. *Metrologia* 32, 231–244.
- Jousset, P., Mori, H., Okada, H., 2003. Elastic models for the magma intrusion associated with the 2000 eruption of Usu Volcano, Hokkaido, Japan. *J. Volcanol. Geotherm. Res.* 125, 81–106.
- Longman, I.M., 1959. Formulas for computing the tidal acceleration due to the Moon and the Sun. *J. Geophys. Res.* 64 (12), 2351–2355.
- Merriam, J.B., 1992. Atmospheric pressure and gravity. *Geophys. J. Int.* 109, 231–244.
- Munk, W.H., Cartwright, D.E., 1966. Tidal spectroscopy and prediction. *Philos. Trans. R. Soc. Ser. A* 259, 533–581.
- Scintrex Operation Manual, 2014. CG-5 Scintrex AutogravTM System. Scintrex Ltd, Concord, Ontario.
- Singh, B., Guptasarma, D., 2001. New method for fast computation of gravity and magnetic anomalies from arbitrary polyhedral. *Geophysics* 66 (2), 521–526.
- Torge, W.T., 1989. *Gravimetry*. Walter de Gruyter, New York, Berlin, p. 465.
- Van Camp, M., 2003. Efficiency of tidal corrections on absolute gravity measurements at the Membach station. Proceedings of the workshop: IMG-2002 Instrumentation and Metrology in Gravimetry. Cahiers du Centre Européen de Géodynamique et de Séismologie, Luxembourg, 22, pp. 99–103.